RED CELL AND GHOST VISCOELASTICITY

Effects of Hemoglobin Concentration and In Vivo Aging

GERARD B. NASH AND HERBERT J. MEISELMAN
Department of Physiology and Biophyics, University of Southern California School of Medicine, Los Angeles, California 90033

ABSTRACT To assess the influence of intracellular hemoglobin concentration on red cell viscoelasticity and to better understand changes related to in vivo aging, membrane shear elastic moduli (μ) and time constants for cell shape recovery (t_c) were measured for age-fractionated human erythrocytes and derived ghosts. Time constants were also measured for osmotically shrunk cell fractions. Young and old cells had equal μ, but t_c was longer for older cells. When young cells were shrunk to equal the volume (and hence hemoglobin concentration and internal viscosity) of old cells, t_c increased only slightly. Thus membrane viscosity ($\eta = \mu \cdot t_c$) increases during aging, regardless of increased internal viscosity. However, further shrinkage of young cells, or slight shrinkage of old cells, caused a sharp increase in t_c. Because this increased t_c is not explainable by elevated internal viscosity, η increased, possibly due to a concentration-dependent hemoglobin-membrane interaction. Ghosts had a greater μ than intact cells, with proportionally faster t_c; their membrane viscosity was therefore similar to intact cells. However, the ratio of old/young membrane viscosity was less for ghosts than for intact cells, indicating that differences between young and old cell η may be partly explained by altered hemoglobin-membrane interaction during aging. It is postulated that these changes in viscoelastic behavior influence in vivo survival of senescent cells.

INTRODUCTION

It is generally agreed that the ability of red cells to deform and alter their shape (i.e., cellular deformability) depends on the following four factors: the membrane mechanical properties, the cytoplasm viscosity, the overall cell shape, and the surface-area-to-volume ratio (Meiselman, 1981; LaCelle, 1972). However, the relative importance of these factors is not clear in all cases. The elastic behavior of the cell is mainly determined by the membrane shear elastic modulus (μ, resistance to shear deformation at constant area), as the membrane resistance to bending is comparatively small (Evans 1980). The membrane is extremely resistant to area dilation (Evans et al., 1979), but the cell can deform greatly without change in area because of its large excess surface. The time-dependent deformation of the erythrocyte is a function of its viscous as well as elastic properties, and these can be assessed by observation of the shape recovery of deformed cells (Hochmuth et al., 1979, 1980). Hochmuth et al. (1979) have shown theoretically that the time constant (t_c) for this essentially exponential recovery process is defined by the membrane surface viscosity (η) and shear elastic modulus (i.e., $t_c = \eta/\mu$), assuming negligible energy dissipation in the cytoplasm and surrounding fluid. This assumption was theoretically verified for values of cytoplasm viscosity typical for normal cells. However, the viscosity of hemoglobin (Hb) solutions increases very rapidly with concentration at values near and above physiologically normal (Cokelet and Meiselman, 1968; Ross and Minton, 1977). In addition, Hb may bind to the membrane and influence cell flexibility (Salhany and Gaines, 1981), and it is possible that this Hb-membrane interaction is concentration dependent. Thus, although the membrane's intrinsic viscoelastic properties are mainly determined by its underlying protein network (Evans and LaCelle, 1975; Evans and Skalak, 1980; LaCelle and Kirkpatrick, 1975), these properties may be influenced by alterations in the cytoplasmic state.

During in vivo aging, erythrocyte deformability becomes impaired (see Nash and Meiselman, 1981, for a recent review of changes in cell mechanical properties with age). Each of the four factors listed above has been claimed to vary with cell age and thus possibly affect in vivo survival (Canham, 1969; LaCelle et al., 1973; Heusinkveld et al., 1977; Williams and Morris, 1980). However, in previous studies, we have shown that the shear elastic modulus of the red cell membrane does not increase significantly during aging (Nash and Wyard 1981 *a*) and also that the observed changes in cell surface area and volume should not impair the ability of aged cells to negotiate the microcirculation (Nash and Wyard, 1981 *b*). More recent investigations (Linderkamp and Meiselman, 1982) have corroborated these findings and further shown that, along with a reduced swelling capacity, older cells require a

longer time for viscoelastic shape recovery. The latter result was attributed to increased membrane surface viscosity, since the elastic modulus is constant. However, as noted above, increases in intracellular Hb concentration (i.e., mean cell hemoglobin concentration, MCHC), which occur during aging, may retard the recovery process.

The aim of the present study was to investigate the influence of the cytoplasm on the viscoelastic properties of human erythrocytes and to better understand the underlying causes of alterations in mechanical behavior that occur during in vivo aging. Specifically, we have measured the effects of changes in Hb concentration on the rate of red cell shape recovery. Density-fractionated, and hence age-fractionated samples (Prankred, 1958; Borun et al., 1957), were compared as a function of hyperosmotic shrinkage. The viscoelastic properties of essentially Hb-free membrane ghosts and intact cells of differing age were also compared, under isotonic conditions, in an attempt to define the properties of the membrane with minimal Hb interaction. Although ghost preparations are widely used for studies of membrane transport, few reports exist of their mechanical properties. Some experiments on the viscosity of bulk suspensions of ghosts have been carried out (Usami and Chien, 1973; Tillman et al., 1980), and limited reports exist on ghost membrane elastic properties (Weed et al., 1969; Heuskinveld et al., 1977). We are not aware of any published data on ghost shape recovery or on comparisons of individual ghosts derived from age-fractionated samples. It is clearly of interest to characterize such ghost preparations as they should provide a useful model for studies of the structural determinants of membrane physical properties.

METHODS AND ANALYSIS

Sample Preparation

Density Fractionation and Osmotic Shrinkage. Blood was obtained from healthy, adult laboratory personnel via venipuncture into heparin (5 IU/ml) and used on the day of withdrawal. Density frationation was based on the method of Laczko et al. (1979). Whole blood was centrifuged at 2,000 *g* for 10 min and a portion of the plasma was reserved for later use. The cells were resuspended in the remaining plasma at 70–80% hematocrit (hct) and loaded into narrow glass tubes (internal diameter 2 mm). The tubes were then sealed at one end and centrifuged at 12,000 *g* for 15 min at room temperature. Cells from the top and bottom 5% of the resulting packed cell column (i.e., young and old cells, respectively) were separated from the mid portion by cutting the tube appropriately. These cells were suspended at $\sim 10^7$ cells/ml in isotonic phosphate buffered saline (PBS, 0.122 M NaCl, 0.030 M KH_2PO_4 + Na_2HPO_4 with 2 mg/ml glucose) containing 0.2% by weight in grams human serum albumin (pH 7.44, 300 mOsmol/kg). If unfractionated cells were to be examined, whole blood was diluted in PBS to the same concentration.

Cells in suspension were osmotically shrunk by addition of a 1 osM NaCl solution. The amount required for a given shrinkage was predicted from published relations of cell volume to medium osmolality (Linderkamp and Meiselman, 1982). Final medium osmolality was measured using a freezing point osmometer (model 2007, Precision Systems, Inc., Sudbury, MA). Cell volumes in the various osmolality media were measured using an Electrozone Celloscope (Particle Data, Inc. Elmhurst, IL, model 112 LA/ADCW) operating with a 20% rejection level to eliminate the artifact caused by nonaxial transit of red cells (Corry et al., 1980). Cell volume in isotonic medium was used to assess the efficiency of the age-fractionation procedure and to characterize the ghost preparations. Red cell and ghost diameters were measured microscopically from video recordings (see below), using a stage micrometer for calibration.

Ghost Preparation. A method similar to that recommended by Schwoch and Passow (1973) for preparation of resealed ghosts in isotonic media was used. However, more dilute cell suspensions were used (to minimize residual Hb content) and adenosine triphosphate (ATP) was included in the lysing medium to improve the yield of disk-shaped ghosts (at the expense of echinocytic shapes). Cells were only briefly exposed to hypotonic conditions at 0°C, minimizing solubiliztion of spectrin.

Whole blood was centrifuged (2,000 *g*, 10 min) and the plasma and buffy coat remove. The cells were washed three times in PBS and finally suspended at 12.5% hct in the same buffer. When ghosts were prepared from young and old cells, the separated samples were washed once in a large excess of buffer and suspended in 1 ml PBS (hct 5–10%). Lysis was induced by adding 1 ml of ice cold cell suspension to 30 ml of 0°C, dilute phosphate buffer (0.010 M KH_2PO_4 + Na_2HPO_4, pH 7.4) containing 0.004 M $MgSO_4$ and 0.5 mg/ml ATP (final buffer was ~30 ideal mOsmol/kg and the hemolysate 40 ideal mOsmo kg). After 5 min at 0°C, the lysate was returned to isotonicity by addition of 7 ml of five-times-concentrated PBS. Resealing of ghosts was facilitated by incubation of this suspension at 37°C for 1 h. The ghosts were centrifuged at 20,000 *g* for 10 min, the supernatant removed, and the pellet washed once in a large excess of PBS. The ghosts were finally suspended in PBS containing albumin and their morphology was assessed by phase-contrast microscopy. For biochemical comparison (see below) with these resealed ATP-ghosts, ghosts were also prepared by the method of Dodge et al. (1963), which involves repeated washing and final suspension of ghosts in a hypotonic phosphate buffer (0.010 M KH_2PO_4 + Na_2HPO_4, pH 7.4).

Hemoglobin and Membrane Protein Analysis

Red cell hemoglobin content was measured by the cyanmethemoglobin method, and the quantity of residual Hb in the ghosts was analyzed by the pyridine hemochromagen technique of Dodge et al. (1963). Total ghost protein was determined by the method of Lowry et al. (1951). Membrane protein components were analyzed by polyacrylamide gel electrophoresis (PAGE), using the method of Laemli et al. (1970).

Determination of Viscoelastic Characteristics

The viscoelastic behavior of red cells and ghosts was characterized by measuring their time constant for shape recovery (t_c) and membrane shear elastic modulus (μ). The membrane surface viscosity (η) was then calculated from the relation $\eta = \mu \cdot t_c$ (Hochmuth et al., 1979). All measurements were carried out at room temperature (24° ± 1°C). Note that for ghost studies, data were collected only for disk-shaped ghosts with morphology similar to biconcave intact cells. For hypertonically shrunk intact cells, t_c measurements were only made on flat, disk-shaped cells. Some of these had slightly irregular outlines, but cells with more abnormal shapes were avoided.

Time Constant for Shape Recovery. Viscoelastic recovery of cell shape was measured and analyzed by the method of Hochmuth et al. (1979). The micropipette and microscope/video systems were as recently described (Linderkamp and Meiselman, 1982), except that in the present study a Zeiss 40x, NA 0.75, long working distance, water-immersion, phase-contrast objective was used. Bright-field optics

were used for intact cells, whereas phase-contrast optics were used for ghost observations. The red cell or ghost suspensions were placed in a chamber made of a standard glass microscope slide and coverslip separated by a U-shaped, 1-mm thick Parafilm (American Can Co., Greenwich, CT) gasket. The chamber was inverted and cells allowed to settle and attach to the coverslip for 10–15 min (30 min for ghosts). The remaining suspension was removed, and the chamber was flushed and finally filled with PBS containing autologous plasma (9% vol/vol). The chamber was then turned right-side up and viscoelastic shape recovery was measured for cells that were point attached to the upper surface. At a point on the cell rim diametrically opposite the attachment, a membrane tongue was sucked into a 1.0–1.5 μm ID micropipette. The cells were extended and subsequently released by withdrawing the pipette; initial deformed cell length/width (L/W) ratio was between 1.5 and 1.8 The presence of plasma in the medium prevented further attachment of cells to the coverslip during relaxation (Hochmuth et al., 1979). From video recordings of the shape recovery process, L/W was measured over a period up to 2 s, initially every 1/60 s, but later at greater intervals.

Using a model of a viscoelastic strip that has undergone uniform extension, the change in cell dimensions can be described by the equation of Hochmuth et al. (1979):

$$\frac{(L/W) - (L/W)^*}{(L/W) + (L/W)^*} \cdot \frac{(L/W)_o + (L/W)^*}{(L/W)_o - (L/W)^*} = \exp(-t/t_c) \quad (1)$$

where $t_c = \eta/\mu$. The ratio L/W refers to the cell dimensions at time t the subscript o refers to the ratio at the first data point ($t = 0$), and the * refers to the ratio at its final value. A more exact analysis for a disk-shaped body, predicts a similar variation in cell shape with time (Hochmuth et al., 1979).

To fit the measured dimensions to the above equation require knowlege of $(L/W)^*$. A value can be assigned, at some time $>>t_c$, and the data fitted to obtain a value for t_c, using a least-squares linear regression of the logarithm of Eq. 1. However, the resulting time constant will be unduly influenced by the data for long time periods (Hochmuth et al., 1980) and will depend on the choice of $(L/W)^*$. Alternatively, optimal values for both t_c and $(L/W)^*$ can be calculated numerically, to minimize the deviation of the experimental data from the model theory (Hochmuth et al., 1979). In this study the latter approach was used. Results were still found to be influenced by the choice of time at which data analysis was terminated (up to 2 s in this study). Thus, the effect of varying the analysis period was investigated, and, for comparison, the linear regression method was evaluated in some experiments.

Membrane Shear Elastic Modulus. A parallel-plate flow-channel technique similar to that of Hochmuth and Mohandas (1972) was used to measure membrane shear elastic modulus. This method was used because micropipette aspiration, which we have previously used to compare young and old intact cells (Nash and Wyard, 1981 *a*; Linderkamp and Meiselman, 1982), was inappropriate because of optical difficulties in observing membrane tongues drawn up from Hb-deficient ghosts. Red cells and ghosts in suspension were allowed to settle onto and attach to the upper glass surface of a rectangular channel. They were subsequently deformed by the forced flow of PBS containing autologous plasma (9% vol/vol). The fluid shear stress at the wall (t_w) was calculated from the known volumetric flow rate (Harvard Apparatus Co., Natick, MA, model 935, variable speed infusion pump driving a 10 ml glass syringe, Hamilton Co., Reno, NV, series 1000) and measured chamber dimensions. Only point-attached cells were chosen for measurement (i.e., attachment region approximately equal to the optical resolution of the system) and their deformation was recorded using the microscope/video system. For each cell or ghost, the ratio of deformed length to initial length (L/L_o) was measured at four shear stresses up to 1 dyn/cm^2. Fig. 1 shows a deformed cell in the flow channel and typical data for L/L_o plotted as a function of $t_w \cdot R$ (R is the undeformed cell radius). For the relatively low shear stresses used, the increase of length

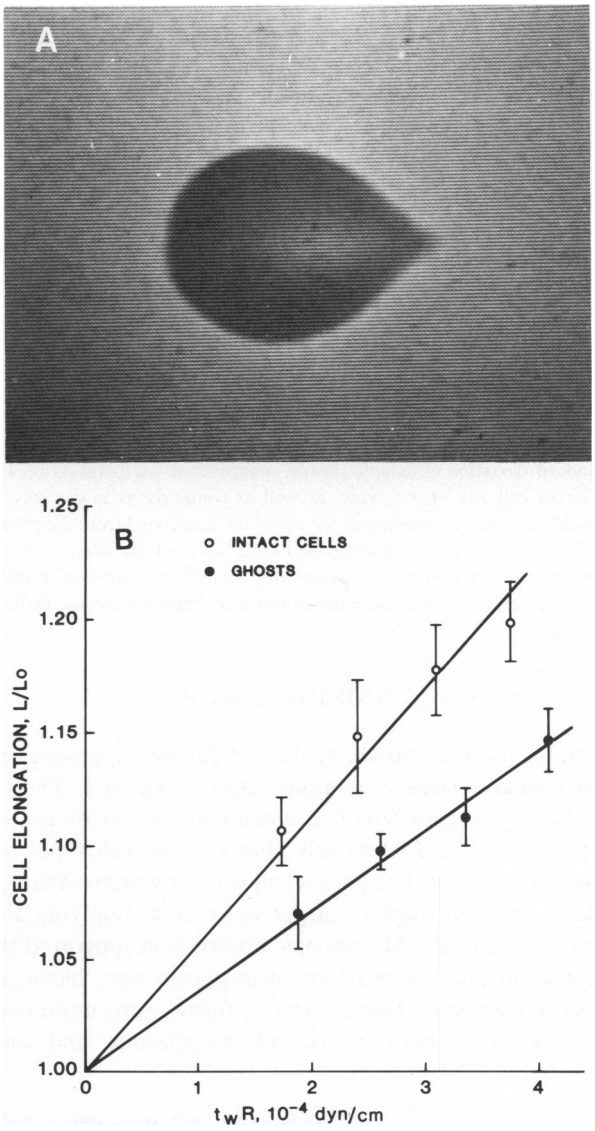

FIGURE 1 (*A*) Photograph of a point-attached red blood cell deformed in the flow channel by a shear stress, t_w, of 1 dyn/cm^2. (*B*) Variation of cell elongation (L/L_o) as a function of $t_w \cdot R$ (R is the undeformed cell diameter). Data are mean ± standard deviation for nine intact unfractionated cells (o) and for eight ghosts derived from unfractionated cells (•); both intact cells and ghosts were from a single donor.

ratio was approximately linear; curvature becomes more evident if greater stresses are applied (Corry et al., 1980).

A theoretical analysis of this system has been made by Evans (1973 *a*, *b*). The red cell was treated as a point-attached flat disk made up of a two-dimensional, incompressible material, deformed by an applied shear stress. A derived stress-strain law was used to predict the nonuniform membrane extension ratio over the disk surface. The extension ratio approached infinity at the attachment point, where the deformed cell width tended to zero. To simulate microscopic observations, Evans (1973 *b*) numerically integrated the membrane extension up to the point where the attachment width fell below the optical diffraction limit (0.5 μm). This integration predicted that the ratio L/L_o would increase in a nearly linear manner as a function of the dimensionless parameter $t_w \cdot R/\mu$. We have found that analysis of our experimental flow-channel data (e.g., Fig. 1) using this theory yielded elastic modulus values much lower than those obtained by micropipette analysis. For example, flow-channel μ values for unfractionated cells averaged 1.8×10^{-3} dyn/cm,

compared with $\sim 6 \times 10^{-3}$ dyn/cm previously reported using micropipette analysis (Waugh and Evans, 1979). This disparitry is most likely due to the approximations inherent in the flow-channel theory. Because micropipette measurements represent generally accepted values, flow-channel data are probably best interpreted in relative terms.

Flow-channel cell elongation data obtained in the present study did follow a linear trend (e.g., Fig. 1), in accordance with the theoretical predictions. Thus, for each cell, the reciprocal of the slope, calculated by linear regression of L/L_o against $t_w \cdot R$, was used as a measure of relative membrane shear elastic modulus; correlation coefficients for these linear regressions averaged between 0.98 and 0.99. For each sample of cells, the mean of the inverse of the slopes and its coefficient of variation were calculated. From repeated experiments, the mean and standard deviation of these means were determined. The results for fractionated intact cells and for ghosts were expressed relative to the mean value for the unfractionated intact cell samples. The latter thus acted as controls and had elastic modulus normalized to unity. As all data represent mean and standard deviation of sample means, independent comparisons between different cell and ghosts types, as well as comparisons to controls, are possible. Similarly, membrane viscosity data, calculated from the product of flow-channel elastic modulus and time constant for shape recovery, were expressed relative to the mean value for unfractionated cell samples. Again, independent standard deviations were retained for the different cell types.

RESULTS AND DISCUSSION

Data for the size and Hb content of density separated cells and derived ghosts are summarized in Table I. The top fraction (younger) cells had mean volumes ~15% greater than the bottom (older) cells, but the two cell types had equal Hb content. The ghosts had smaller volumes than the intact cells but slightly larger diameters, implying that they were thinner. Microscopic observation supported this impression and showed that most ghosts were biconcave disks. Cup-shaped (stomatocytic) forms were more common in ghosts than in red cell suspensions, and some echinocytic ghosts were present. The latter occurred in greater numbers if ATP was omitted from the preparation. Approximately 1% of the original Hb was left in the ATP-ghosts, compared with 0.5% in the ghosts prepared by the method of Dodge et al. (1963). Total ghost protein was greater for the ATP-ghosts (9.4×10^{-13} g/ghost vs. 7.1×10^{-13} g/ghost for the Dodge preparation), probably because of their greater Hb content. Polyacrylamide gel electrophoresis (PAGE) showed no differences in protein profiles between ghosts prepared by either method nor between ghosts prepared from young and old cells.

Viscoelastic properties of intact cells are shown in Table II. Membrane shear elastic modulus was measured using the flow channel, and values are expressed relative to control unfractionated red cells. Data obtained in earlier micropipette studies (Nash and Wyard, 1981 *a*; Linderkamp and Meiselman, 1982) are also shown. Comparative values for the different samples are consistent by both techniques. The data show that membrane elasticity does not change significantly during in vivo aging. Disparity in absolute μ values obtained by the two methods (see Methods) partly arises from underestimation of the deforming force applied to cells in the flow channel (Meiselman et al., 1978; Waugh and LaCelle, 1980). In the theoretical model used to analyze the flow-channel data, the total force on the cell is the shear stress multiplied by its undeformed projected area. In fact, the true drag on a cell is expected to be greater because of its finite thickness. It has been shown, for example, that the drag on a hemispherical particle is four to five times that experienced by a disk of equal projected area (Hyman, 1972 *a*, *b*). Thus, the force required for a given cell elongation is underestimated and the elastic modulus undervalued. However, we suggest that

TABLE I
SIZE AND HEMOGLOBIN CONTENT OF RED CELLS AND GHOSTS*

	Mean cell volume	Diameter	Hemoglobin
	(μm^3)	(μm)	(10^{-13} g/cell)
Red Cells			
Unfractionated	90 ± 4.5 (4) (17%)	8.25 ± 0.32 (4) (4.5%)	309 ± 15 (6)
Top fraction	96 ± 2.0 (10) (18%)	8.4 ± 0.26 (10) (4.0%)	298 ± 6 (3)
Mid fraction	89 ± 1.5 (5) (17%)	7.9 ± 0.12 (5) (4.5%)	—
Bottom fraction	82 ± 2.0 (10) (18%)	7.7 ± 0.29 (10) (4.5%)	303 ± 8 (3)
Ghosts			
Unfractionated	67 ± 3.0 (9) (22%)	8.5 ± 0.27 (9) (5.0%)	2.5 ± 0.5 (4)‡
Top fraction	68 ± 3.0 (7) (24%)	8.9 ± 0.16 (8) (4.0%)	3.2 ± 2.0 (2)
Bottom fraction	63 ± 2.5 (7) (23%)	8.25 ± 0.23 (8) (4.5%)	2.4 ± 1.3 (2)

*Values are the mean ± standard deviation from (n) experiments. Percentages in parentheses represent the averages of the coefficients of variation in these n experiments. For the diameter values, 16 red cells and 10–12 ghosts were measured in each experiment.
‡Unfractionated ghosts prepared by the method of Dodge et al. (1963) contained $1.4 \pm 0.5 \times 10^{-13}$ g Hb/ghost (three experiments).

the method is useful for comparison of the membrane elastic modulus of similarly shaped cells. Previous flow-channel data for cell elongation have been presented by Hochmuth and Mohandas (1972), both for point attached cells and for cells with a 2–3 μm width of attachment. They found that smaller widths of attachment produced greater extensions at a given shear stress. Our extension data for point attached cells agree with the results of Hochmuth and Mohandas (1972), but were limited to a lower range of shear stresses where L/L_o increased nearly linearly. As the extensional behavior was close to that predicted by the theory of Evans (1973 *a*, *b*), relative μ values were calculated from a linear approximation. The validity of the flow channel measurement of membrane elasticity is discussed in greater detail below.

Older cells recover their shape more slowly than younger cells (Table II, column 4). Differences in t_c between young and old cells were significant ($p < 0.01$) in each experiment. Values for the membrane surface viscosity ($\eta = \mu \cdot t_c$) are shown in columns 5 and 6, using the flow-channel and micropipette values for μ, respectively. The latter η values are similar to previously published results (Hochmuth et al., 1980; Linderkamp and Meiselman, 1982). Clearly, membrane viscosity increases during aging if one assumes that increased MCHC contributes negligibly to the measured t_c values.

The t_c values shown in Table II are slightly greater than in previously published results (Hochmuth et al., 1980; Linderkamp and Meiselman, 1982). In fact, the time constants are influenced by the method of analysis and the period for which L/W is measured. Those shown were obtained by analyzing shape recovery for 0.5 s after cells were released, using the two-parameter (t_c and L/W^*) fit of Hochmuth et al. (1979). If data for up to 2 s were included, then time constants were longer by ~0.2 s. Conversely, if the data were truncated further, smaller values were obtained. When values for t_c were calculated from linear regression of the logarithm of Eq. 1, they were strongly influenced by the choice of the final L/W, i.e., $(L/W)^*$. If data for longer times were included, greater t_c values were obtained. However, the large differences in t_c between young and old cells were evident regardless of the analysis procedure.

The reason for the dependence of t_c values on the period for which shape recovery is measured can be clarified if the experimental data are plotted on log-linear graph paper using Eq. 1. The curve is found to deviate from linearity after two or three time constants, with the rate of shape recovery then slowing down. Hochmuth et al. (1980) state that at long time periods data might not fit their planar viscoelastic approximation because of the effects of "bending (curvature elastic energy)" and the possibility of permanent plastic flow at the cell tips. In addition, Fischer et al. (1981) have suggestd that the membrane shear elastic modulus may be strain dependent, with a lower value at smaller strains. Thus, as cells approach their resting shape, the restoring force might decrease, contributing to a decrease in their recovery rate. If the membrane elasticity is strain dependent, this might also be reflected in the relation of cell elongation to applied stress in the flow channel and might influence the μ values calculated. The effect is only expected to be noticeable at low strains (i.e., <1.3, Fisher et al., 1981). Although overall cell elongation in the flow channel was only ~10–20%, the membrane extension ratio is not constant over the cell surface (Evans, 1973 *b*). It rises rapidly in the attachment region where

TABLE II
VISCOELASTIC PROPERTIES OF INTACT RED BLOOD CELLS

	Membrane shear elastic modulus, μ			Time constant for Shape recovery, t_c*	Membrane Surface Viscosity, η*	
	Flow channel (relative to control)*	Micropipette‡ (a)	Micropipette‡ (b)		(*a*) (relative to control)	(*b*)
		(10^{-3} dyn/cm)		(s)		(10^{-4} dyn · s/cm)
Unfractionated control cells	1.00 ± 0.10 (4) (13%)	—	6.0 ± 1.1	0.15 ± 0.01 (4) (19%)	1.00 ± 0.13 (23%)	9.0
Top fraction	1.00 ± 0.06 (4) (12%)	5.8 ± 0.7	5.5 ± 0.9	0.13 ± 0.01 (11) (17%)	0.87 ± 0.08 (21%)	7.2
Mid fraction	—	—	—	0.15 ± 0.01 (5) (19%)	—	—
Bottom fraction	1.06 ± 0.06 (4) (14%)	6.0 ± 1.1	6.4 ± 1.1	0.19 ± 0.02 (11) (19%)	1.32 ± 0.16 (24%)	12.2

*Values are the mean ± standard deviation of sample means from (*n*) experiments. Percentages in parentheses represent the average sample coefficients of variation. In each experiment 8–10 cells were measured. Flow-channel elastic modulus values are expressed relative to the mean value for unfractionated cells, which was itself normalized to unity. For t_c, experimental data were analysed for 0.5 s after the cells were released, using the two-parameter [t_c and $(L/w)^*$] fit of Hochmuth et al. (1979).

‡Data from previous studies using micropipette analysis; (*a*) Nash and Wyard, 1981 *a* (*b*) Linderkamp and Meiselman, 1982.

§Values represent the mean ± standard deviation, and typical sample coefficient of variation, calculated as the product of the tabulated time constant and elastic modulus from (*a*) flow channel and (*b*) micropipette analysis (Linderkamp and Meiselman, 1982). The mean η values derived using the flow-channel elastic modulus are expressed relative to the mean value for unfractionated cells, which was again normalized to unity.

most of the cell elongation actually occurs. Thus, neither slight curvature in the relation of L/L_o to $t_w \cdot R$ (Fig. 1 *B*) nor low calculated μ values can be clearly assigned to the effect of a strain-dependent elastic modulus. It is more likely that nonlinearity in L/L_o at high stresses results from a gradual departure from the theoretical model, arising from increasing curvature of the membrane in the attachment region (Evans, 1973 *b*). Under these circumstances forces normal to the membrane, ignored in the model calculations, are expected to become important.

It is not clear to what extent the internal Hb concentration influences red cell viscoelastic behavior. To evaluate this, the effect of osmotic cell shrinkage on the rate of shape recovery was studied. Because older cells have higher MCHC and hence higher internal viscosity, young cell fractions were shrunk to have mean volumes and MCHC levels equal to old cell fractions. This caused only a small increase in young cell t_c (10 ± 5%, four experiments). Subsequently, when older cells were swollen to equal younger cells, recovery time decreased by a similar percentage (8 ± 3%, two experiments). However, further shrinkage of young cells or quite small decreases in old cell volume caused t_c to increase markedly. The variation in t_c (relative to its value in isotonic medium) as a function of decreasing cell volume is illustrated in Fig. 2. Note that a 10% decrease in old cell volume causes t_c to approximately double, whereas smaller increases are observed for the young and unfractionated cells. These data thus show that at values close to, but above the normal physiological level, MCHC strongly influences the rate of shape recovery.

Only disk-shaped shrunken cells were measured for the experimental data shown in Fig. 2. Elongation of more irregularly shaped cells would initially be taken up in straightening out their buckled regions. The later stages of shape recovery for such cells would then be dominated by restoration of curvature, which is expected to be a relatively slow process. In the present study, shrunken cell relaxation followed a slower course, divergent from that of control cells throughout the entire recovery process and not just toward its end. Their time constants were longer than for controls, even if data were truncated so that only the initial part of the shape recovery was analyzed. Thus, changes in cell shape were not responsible for the increased t_c values for shrunken cells.

The curves in Fig. 2 seem to imply that the internal Hb concentration has more influence on the viscoelastic behavior of old cells than young ones. However, the different fractions have unequal MCHC in isotonic media (i.e., older cells have a higher MCHC). The data can be replotted as a function of MCHC (Fig. 3 *A*) using the known isotonic hemoglobin concentrations. The data in Fig. 3 *A* thus show the time constants relative to the isotonic value for each fraction, but do not have a common MCHC intercept. To express these data relative to a common origin of 31 g/dl (i.e., the MCHC of young cells in isotonic media), the old and unfractionated data were

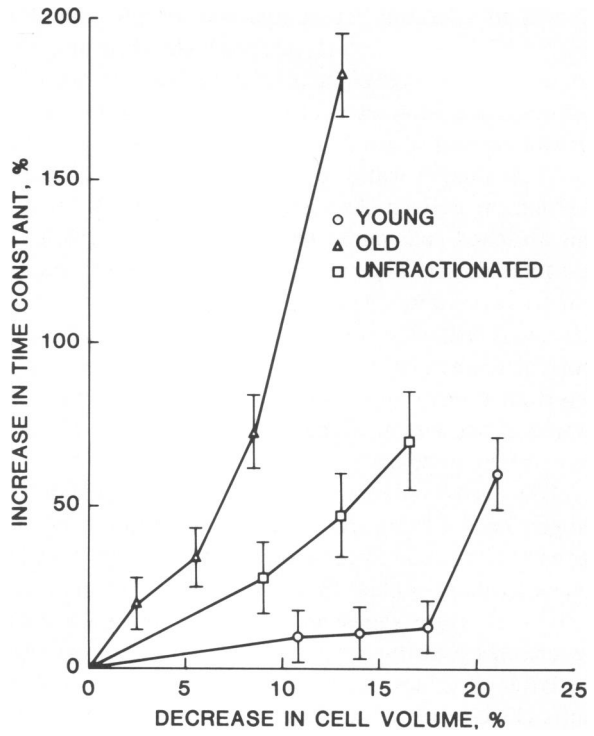

FIGURE 2 Effect of cell shrinkage on the time constant for viscoelastic shape recovery (t_c). The time constant increases as cell volume decreases; old cells (Δ) undergo a more rapid increase in t_c compared with unfractionated (□) or young (○) cells. Each point represents at least two experiments, on different donors, in which shrunk cells were compared to cells in isotonic medium. In each experiment a ratio of the mean time constants were calculated (shrunken/isotonic cells). These ratios were averaged for the different donors so that the percent increase in t_c could be calculated. Bars represent the standard error for the ratio in a typical experiment in which 8–10 cells of each type were measured.

corrected for the effect of swelling on t_c: (*a*) because swelling old cells to equal young cell volume decreased t_c by 8%, the relative t_c values for old cells were multiplied by 1.08; (*b*) the unfractionated data were multiplied by an intermediate factor of 1.04. The results of these computations are shown in Fig. 3 *B*, where it can be seen that the proportional change in t_c as a function of MCHC is similar for all cell fractions. Note that these graphs do not show the constant underlying differences in absolute t_c values between the cells of different age. These differences are attributed to unequal membrane viscosity at all Hb concentrations.

To test the membrane properties relatively free from the influence of Hb, ghosts prepared from different cell fractions were used (see Table III). In the flow channel, ghost elongation as a function of shear stress followed the same pattern as for intact cells. However, the slope of this relation and the final ghost elongation were less, so that ghosts had greater elastic moduli than intact cells. It is important to ascertain that these differences are genuine reflections of membrane properties and that they do not arise from experimental artifacts associated with the approximations in the theory and in our data analysis. As

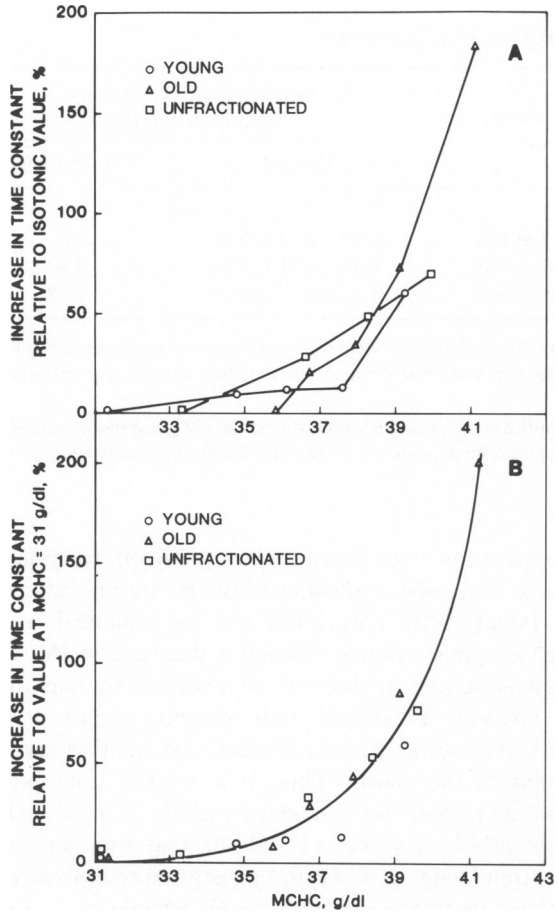

FIGURE 3 Relative t_c values replotted as a function of MCHC. (*A*) For each fraction, t_c is expressed relative to its value in isotonic medium. The curves do not have a common origin since isotonic MCHC is not the same for the three fractions. (*B*) By allowing for the effect of cell swelling on t_c, all time constants are expressed relative to their values at MCHC 31 g/dl (see text). The single hand-fitted line appears to describe the data for all samples.

noted earlier, modeling red cells as flat disks leads to underestimation of drag applied in the flow channel, which may explain the low μ values obtained, compared with micropipette measurements. Because ghosts had lower volumes than the intact cells, we tested the effect of swelling ghosts to the same volume as intact cells. In three experiments this had no significant effect on their measured relative μ values. It therefore appears that the cell surface area and/or depth of protrusion into the flow are of more direct importance than the cell volume in determining the drag acting on the cell. Swelling the ghosts probably caused the dimple regions to fill out, with minimal effect on the maximum thickness at their edges. Thus the decreased volume of ghosts compared with intact cells was not the cause of their unequal μ values, presumably because their surface areas and overall shapes were so similar.

Another possible artifact is the linear approximation that was applied to the analysis of the flow channel data. However, this approximation did not differentially bias the relative μ values obtained for ghosts vs. intact cells. The same stresses were applied to both preparations and the lines for L/L_o vs. $t_w \cdot R$ were divergent over the entire stress range. Linear regression analysis of different portions of the curves yielded slightly different slopes, but did not significantly change the ratio of ghost/intact cell values. Finally, the flow-channel data did not show clear evidence of a strain-dependent membrane elastic modulus. Such strain-dependent behavior would not, in any case, explain the inequality of ghosts and intact cells as the latter experienced greater strains and would hence appear stiffer. We conclude that the flow-channel technique is valid for measuring membrane elasticity as long as the applied stresses are low enough to cause an approximately linear cell elongation response and attention is paid to the possible influence of cell geometry. Thus, the higher elastic moduli measured for ghosts do reflect their greater membrane stiffness compared to intact cells.

The reason for the increased ghosts elastic modulus is not clear, since it seems unlikely that it would result from the loss of Hb. We note that (*a*) treating ghosts with reducing agents (0.01 M sodium sulfite or 0.005 M dithiothreitol) did not decrease their elastic modulus. These agents would tend to break spontaneously formed disulphide–cross-linked proteins, which might otherwise have affected the membrane elasticity (Fischer et al., 1978 *a*). (*b*) Preparation and measurement of ghosts in the presence of EDTA (0.5 mg/ml had no effect on deformation in the flow channel. Calcium-mediated cross-linking of proteins (Lorand et al., 1976) would be inhibited by this procedure.

Table III also shows ghost time constants and the calculated membrane viscosities for both ghosts and intact cells. The membrane viscosities are all expressed relative to the mean value for control unfractionated intact cells. In general, the time constants were faster for ghosts than for intact cells, changing in proportion to the increased ghost elastic modulus. Thus the membrane viscosity was similar for ghosts and intact cells. Values for η were nearly unchanged for young ghosts, but were lower for old ghosts than intact cells. Thus, when ghosts from young and old cells were compared, the differences in relative membrane viscosity were smaller than for intact cells. If the ratio of old/young ghost membrane viscosity was calculated for each of the four donors tested, the result was 1.23 ± 0.05 (significantly greater than 1.0, $P < 0.01$, but less than the ratio of 1.51 ± 0.22 for intact cells, $P < 0.025$).

CONCLUSIONS

Separation of top and bottom fractions from a centrifuged, packed cell column has enabled us to compare the viscoelastic properties of relatively young and old intact erythrocytes and ghosts. In agreement with previous studies of intact cells (Nash and Wyard, 1981 *a*; Linderkamp and Meiselman, 1982), we found that the membrane shear elastic modulus did not vary significantly with cell age but

TABLE III
VISCOELASTIC PROPERTIES OF MEMBRANE GHOSTS*

	Shear elastic modulus (relative to control)	Time constant for shape recovery	Membrane surface viscosity (relative to control)	
			Ghosts‡	Intact Cells§
		(s)		
Unfractionated ghosts	1.68 ± 0.17 (15%)	0.084 ± 0.01 (14%)	0.92 ± 0.11 (20%)	1.0
Young ghosts	1.71 ± 0.25 (13%)	0.077 ± 0.01 (14%)	0.85 ± 0.20 (18%)	0.87
Old ghosts	1.93 ± 0.31 (15%)	0.083 ± 0.005 (14%)	1.04 ± 0.25 (20%)	1.32

*Values are mean ± standard deviation of sample means for four donors followed by the average coefficient of variation in the experiments; 8–11 ghosts were measured in each experiment. Elastic modulus and membrane viscosity data are expressed relative to the mean values obtained for unfractionated control intact cells. The control values were normalized to unity.

‡Because of variability between donors, the averaged data do not show a highly significant difference between young and old ghost membrane viscosity ($0.15 < P < 0.2$). However, if the ratio of old/young ghost membrane viscosity was calculated individually for the four donors, the result was 1.23 ± 0.05, which is significantly greater than one ($P < 0.01$).

§Data from Table II.

that the time constant for shape recovery was 40–50% longer for the older cell fractions than for the younger cells.

Energy dissipation in the cytoplasm during extensional recovery is proportional to the internal viscosity and predicted to be 1% of that dissipated in the membrane (Hochmuth et al., 1979). The viscosity of Hb solutions rises rapidly as a function of concentration at values near and above those physiologically normal (Cokelet and Meiselman, 1968; Charache et al., 1967). Even though internal viscosity is expected to be much higher for older cells (Williams and Morris, 1980), membrane dissipation should still dominate shape recovery. In fact, when MCHC was equalized, either by shrinking young cells or swelling old cells, only small changes in t_c were observed. It can thus be concluded that the membrane viscosity is higher for older cells, independent of their greater internal viscosity. On the other hand, further shrinkage of young cells or slight shrinkage of old cells resulted in a sharp increase in recovery time. From the theoretical study of Ross and Minton (1977), it can be calculated that the maximally shrunk old cells would have an internal viscosity about five times the normal value. Even so, the internal dissipation would be small (i.e., ~5%) compared with membrane dissipation. Thus it seems that the membrane itself is affected by cell shrinkage, possibly because of increased Hb binding or interaction leading to an increase in η.

Other workers have found that shrinkage impairs cell deformability. Charache et al. (1967) observed that shrunken cells (medium tonicity up to 400 mOsmol/kg) were less filterable through 3–5 μm pores. Clark et al. (1978) found that similar cells elongated less in a Couette viscometer, as estimated by the shape of their light-scattering pattern. In addition, the viscosity of suspensions of osmotically shrunken cells is higher than that for isotonic cells at comparable hematocrits (Schmid-Schönbein et al., 1973; Meiselman, 1978). Our results suggest that these findings may reflect altered membrane properties as well as increased cytoplasm viscosity.

Preparation of ghosts caused a significant, reproducible increase in the shear modulus of the membrane compared with intact cells. This could not be explained by the decreased ghost volume causing a decrease in the shear drag experienced in the flow channel nor by bias in the data analysis. Treatment with reducing agents or with EDTA did not significantly decrease the membrane elastic modulus of the ghosts. Thus, it is unlikely that protein cross-linking had induced ghost rigidity. PAGE showed protein profiles for the ATP ghosts that were similar to those from Dodge et al. (1963) ghosts and resembled those typically reported in the literature (Fairbanks et al., 1971). Previously, Weed et al. (1969) have used micropipettes to test ghost and intact cell elasticity. Ghosts and intact cells behaved similarly. However, for the pipettes used in their study (2.5–3 μm diam), the pressures required to suck up small tongues of membrane were so great as to imply that the elastic moduli were nearly an order of magnitude greater than the normally accepted values from micropipette analysis (Waugh and Evans, 1979). Also using a micropipette method, Heusinkveld et al. (1977) found that ghosts obtained using a one-step procedure, probably with 5–10% residual Hb, had elastic moduli close to intact cells. Few details were given of the ghost characteristics and results obtained, although the elastic moduli were lower than those normally obtained by micropipette analysis. Recently, ghosts prepared by a method similar to that used herein were found to have shorter t_c than intact cells (Dr. R. E. Waugh, personal communication); such a reduction is consistent with our t_c data. In general, because of differences in preparative methodology, it is difficult to compare results between ghost studies. Variations in procedure are known to affect membrane structure and function after hemolysis (Schwoch and Passow, 1973); future studies of the influence of such factors as pH and tonicity on ghost membrane mechanical properties appear warranted.

Although the factors causing the increased ghost shear modulus in our study are not clearly understood, the data do reflect the relative membrane stiffness of the different

ghost populations. Thus, when combined with the t_c measurements, η values for the different age populations can be compared. As would be expected for increased μ, t_c values for all ghosts were shorter than for intact cells such that η was similar for both preparations. However, the difference in η between young and old ghosts was less than between the equivalent intact red cells. Thus, even at physiological concentrations, Hb/membrane interaction may affect membrane viscosity. In particular, the interaction may change during aging so that removal of Hb causes a larger decrease in η for old cells. Most studies of Hb binding to red cell membrane have been carried out using unsealed ghost preparations at low tonicity and low Hb concentration (see Salhany and Gaines, 1981, for review); under these conditions binding is pH and ionic strength dependent. Recently, Hb/membrane interaction has been demonstrated for intact cells under physiological conditions (Eisinger et al., 1982). Salhany and Gaines (1981) suggest that binding of cytoplasmic proteins might affect membrane "flexibility," and our findings add some support to this view. In summary, we propose that a concentration dependent Hb-membrane interaction alters membrane viscosity for cells of all ages, especially above normal MCHC (Fig. 3). Further, based on the ghost data, we suggest that the Hb-membrane interaction may change with cell age, thereby contributing to differences in membrane mechanical properties between young and old cells.

In addition to the possible influence of Hb, alterations in membrane structural proteins might play a part in the membrane aging process, leading to increased membrane viscosity. Although using PAGE we noted no differences between young and old ghosts, comparisons were qualitative rather than quantitative. Previous studies have suggested that the relative quantities of membrane proteins vary with cell age (Kadulbowski, 1978) and that high molecular weight protein aggregates are formed in older cells (Hochstein and Jain, 1981). In addition, Shiga et al. (1979 *a*) found that total membrane protein was constant during aging so that the protein/lipid ratio increased. However, Cohen et al. (1976) noted less membrane protein in older cells.

Whatever the mechanims, it is clear that the viscoelastic characteristics of red cells alter during in vivo aging. Both membrane and internal viscosity increase, the latter because Hb content remains constant while cell volume decreases. Various differences noted in the response of young and old cells to deforming forces (e.g., Shiga et al., 1979 *b*; Pfafferott et al., 1982) can be related to these changes (see Nash and Meiselman, 1981, for review). It is expected that the dynamic behavior of the cells will be affected, rather than their static deformation in response to a constant force. That is, under the influence of a given force, an older cell will take longer to reach its final deformation, or, to reach a given deformation in a certain time, an older cell will require a greater force. This might affect in vivo survival. Because membrane elastic modulus does not change during aging, and because changes in surface area and volume are such that older cells should still be able to pass through narrow pores (Nash and Wyard 1981 *a,b*; Linderkamp and Meiselman, 1982), simple in vivo filtration or trapping of old cells is unlikely to occur. However, if older cells can deform only relatively slowly, we anticipate that they will be delayed in passing through regions of the reticuloendothelial system. This could play a part in their recognition and removal, probably by a more specific immunological mechanism (Kay, 1975, 1978). Note that the bottom fractions tested in this study represent only a relatively old population of cells, which are evidently still viable. Cell volume may continue to decrease and MCHC to increase up to the time of elimination from the circulation. In that case, our data for the effect of osomotic shrinkage suggest that their ability to alter shape rapidly would have become even more impaired.

We also note that the viscous and elastic properties of the membrane combine to make red cell deformation dependent on frequency. Under the influence of a fluctuating force, the extent of deformation should vary according to the frequency of the fluctuation. Slowly varying forces would allow cells to deform fully, but at frequencies $>1/t_c$ cells could not respond adequately and reach full deformation. The frequency response for young and old cells would be slightly different. Experimentally, it has been observed that when red cells are deformed in fluid shear systems, the membrane "tank treads" with a frequency dependent on the suspending fluid shear rate (Fischer et al., 1978 *a*). In these circumstances, some regions of the membrane will experience varying shear deformation (Fischer, 1980). Over the range of shear rates tested (Fischer et al., 1978 *a*) the tank tread frequencies did in fact vary from less than to greater than $1/t_c$. Thus, we expect that the extent of deformation in fluid shear systems depends not only on the shear force applied and the membrane elastic modulus but also on the tank tread frequency and membrane viscosity.

We acknowledge gratefully the technical assistance of Ms. Rosalinda Wenby. We wish to thank Dr. E. A. Evans for the computer program used for the two-parameter fit for the shape recovery data, and Dr. R. Farley for aid in carrying out protein analyses.

This work was supported in part by National Institutes of Health grants HL15722 and HL15162 and by American Heart Association–Greater Los Angeles Affiliate Investigative Award 537IG5.

Received for publication 10 August 1982 and in final form 23 February 1983.

REFERENCES

Borun, E. R., W. G. Figueroa, and S. M. Perry. 1957. The distribution of Fe59 tagged human erythrocytes in centrifuged fractions as a function of age. *J. Clin. Invest.* 36:676–679.

Canham, P. B. 1969. Difference in geometry of young and old cells explained by a filtering mechanism. *Circ. Res.* 25:39–45.

Charache, S., C. L. Conley, D. F. Waugh, R. G. Ugoretz, and J. R. Spurrell. 1967. Pathogenesis of hemolytic anemia in homozygous hemoglobin C disease. *J. Clin. Invest.* 46:1795–1810.

Clark, M. R., N. Mohandas, V. Caggiano, and S. B. Shohet. 1978. Effects of abnormal cation transport on disiccytes. *J. Supramol. Struct.* 8:521–532.

Cohen, N. S., T. E. Eckholm, M. G. Luthra, and D. J. Hanahan. 1976. Biochemical characterisation of density separated human erythrocytes. *Biochim. Biophys. Acta.* 419:229–242.

Cokelet, G. R., and H. J. Meiselman. 1968. Rheological comparison of hemoglobin solutions and erythrocyte suspensions. *Science (Wash., D.C.).* 162:275–277.

Corry, W. D., H. J. Meiselman, and P. Hochstein. 1980. *t*-butyl hydroperoxide-induced changes in the physico-chemical properties of human erythrocytes. *Biochim. Biophys. Acta.* 597–224–234.

Dodge, J. T., C. Mitchell, and D. J. Hanahan. 1963. The preparation and characterisation of hemoglobin-free ghosts of human erythrocytes. *Arch. Biochem. Biophys.* 100:119–130.

Eisinger, J., J. Flores, and J. M. Salhany. 1982. Association of cytosol hemoglobin with the membrane in intact erythrocytes. *Proc. Natl. Acad. Sci. USA.* 79:408–412.

Evans, E. A. 1973 *a*. A new material concept for the red cell membrane. *Biophys. J.* 13:926–940.

Evans, E. A. 1973 *b*. New material concept applied to the analysis of fluid shear- and micropipette-deformed red blood cells. *Biophys. J.* 13:941–954.

Evans, E. A. 1980. Minimum energy analysis of membrane deformation applied to pipet aspiration and surface adhesion of red blood cells. *Biophys. J.* 30:265–284.

Evans, E. A., and P. L. LaCelle. 1975. Intrinsic material properties of the erythrocyte membrane indicated by mechanical analysis of deformation. *Blood.* 45:29–43.

Evans, E. A., and R. Skalak. 1980. Mechanics and Thermodynamics of Biomembranes. CRC Press, Inc., Boca Raton, FL. 1–415.

Evans, E. A., R. Waugh, and L. Melnik. 1979. Elastic area compressibility modulus of red cell membrane. *Biophys. J.* 16:585–595.

Fairbanks, G., T. L. Steck, and D. F. H. Wallach. 1971. Electrophoretic analysis of the major polypeptides of the human erythrocyte membrane. *Biochemistry.* 10:2606–2617.

Fischer, T. M. 1980. On the energy dissipated in a tank-treading human red blood cell. *Biophys. J.* 32:863–868.

Fischer, T. M., C. W. M. Haest, M. Stohr, D. Kamp, and B. Deuticke. 1978 *a*. Selective alteration of erythrocyte deformability by SH-reagents. *Biochim. Biophys. Acta.* 510:270–282.

Fischer, T. M., M. Stohr, and H. Schmid-Schönbein. 1978 *b*. Red blood cell (RBC) microrheology: comparison of the behaviour of single RBC and liquid droplets in shear flow. *Am. Inst. Chem. Eng. Symp. Ser.* 182. 74:38–45.

Fischer, T. M., C. W. M. Haest, M. Stöhr-Liesen, H. Schmid-Schönbein, and R. Skalak. 1981. The stress free shape of the red blood cell membrane. *Biophys. J.* 34:409–422.

Heusinkveld, R., D. A. Goldstein, R. I. Weed, and P. L. LaCelle. 1977. Effect of protein modification on erythrocyte membrane mechanical properties. *Blood Cells.* 3:175–182.

Hochmuth, R. M., and N. Mohandas. 1972. Uniaxial loading of the red cell membrane. *J. Biomech.* 3:501–509.

Hochmuth, R. M., P. R. Worthy, and E. A. Evans. 1979. Red cell extensional recovery and the determination of membrane viscosity. *Biophys. J.* 26:101–114.

Hochmuth, R. M., K. L. Buxbaum, and E. A. Evans. 1980. Temperature dependence of the viscoelastic recovery of red cell membrane. *Biophys. J.* 29:177–182.

Hochstein, P., and S. K. Jain. 1981. Association of lipid peroxidation and polymerization of membrane proteins with erythrocyte aging. *Fed. Proc.* 40:183–188.

Hyman, W. A. 1972 *a*. Shear flow over a protrusion from a plane wall. *J. Biomech.* 5:45–48.

Hyman, W. A. 1972 *b*. Shear flow over a protrusion from a plane wall: addendum. *J. Biomech.* 5:643.

Kadulbowski, M. 1978. The effect of in vivo aging of the human erythrocyte on the protein of the plasma membrane. *Int. J. Biochem.* 9:67–78.

Kay, M. M. B. 1975. Mechanism of removal of senescent cells by human macrophages in situ. *Proc. Natl. Acad. Sci. USA.* 72:3521–3525.

Kay, M. M. B. 1978. Role of Physiologic autoantibody in the removal of senescent human red cells. *J. Supramol. Struct.* 9:555–567.

LaCelle, P. L. 1972. Effect of sphering on red cell deformability. *Biorheology.* 3:51–59.

LaCelle, P. L., and F. H. Kirkpatrick. 1975. Determinants of erythrocyte membrane elasticity. *In* Erythrocyte Structure and Function. G. J. Brewer, editor. Alan R. Liss, Inc., New York. 535–560.

LaCelle, P. L., F. H. Kirkpatrick, M. D. Udkow, and B. Arkin. 1973. Membrane fragmentation and Ca-membrane interaction: potential mechanism of shape change in the senescent red cell. *In* Red Cell Shape. M. Bessis, R. I. Weed, and P. F. Leblond, editors. Springer-Verlag, New York, Inc., New York. 69–78.

Laczko, J., C. J. Feo, and W. Phillips. 1979. Discocyte-echinocyte reversibility in blood stored in CPD over a period of 56 days. *Transfusion (Phila.).* 19:379–388.

Laemli, U. K. 1970. Cleavage of structural proteins during the assembly of the head of the bacteriophage t4. *Nature (Lond.).* 227:660–885.

Linderkamp, O. L., and H. J. Meiselman. 1982. Geometric, osmotic and membrane mechanical properties of density-separated human red cells. *Blood.* 59:1121–1127.

Lorand, L., L. B. Weisman, D. L. Epel, and J. Bruner-Lorand. 1976. Role of the intrinsic transglutaminase in the Ca^{++}-mediated crosslinking of erythrocyte proteins. *Proc. Natl. Acad. Sci. USA.* 73:4479–4481.

Lowry, O. H., N. J. Rosebrough, A. L. Farr, and R. J. Randall. 1951. Protein measurement with the folin phenol reagent. *J. Biol. Chem.* 193:265–275.

Meiselman, H. J. 1978. Rheology of shape-transformed human red cells. *Biorheology.* 15:225–237.

Meiselman, H. J. 1981. Morphological determinants of red cell deformability. *Scand. J. Clin. Lab. Invest.* 41:27–34.

Meiselman, H. J., E. A. Evans, and R. M. Hochmuth. 1978. Membrane mechanical properties of ATP-depleted erythrocytes. *Blood.* 52:499–504.

Nash, G. B., and H. J. Meiselman. 1981. Red cell ageing: changes in deformability and other possible determinants of in vivo survival. *Microcirculation.* 1:255–284.

Nash, G. B., and S. J. Wyard. 1981 *a*. Erythrocyte membrane elasticity during in vivo ageing. *Biochim. Biophys. Acta.* 643:269–275.

Nash, G. B., and S. J. Wyard. 1981 *b*. Changes in surface area and volume measured by micropipette aspiration for erythrocytes ageing in vivo. *Biorheology.* 17:479–484.

Pfafferott, C., R. Wenby, and H. J. Meiselman. 1982. Morphologic and internal viscosity aspects of RBC rheologic behavior. *Blood Cells.* 8:65–78.

Prankred, T. A. J. 1958. The ageing of red cells. *J. Physiol. (Lond.).* 143:325–331.

Ross, P. D., and A. P. Minton. 1977. Hard quasi-spherical model for the viscosity of hemoglobin solutions. *Biochem. Biophys. Res. Commun.* 76:971–976.

Salhany, J. M., and K. C. Gaines. 1981. Connections between cytoplasmic proteins and the erythrocyte membrane. *Trends Biochem. Sci.* 6:13–15.

Schmid-Schönbein, H., R. E. Wells, and J. Goldstone. 1973. Effect of ultrafiltration and plasma osmolarity upon the flow properties of blood. *Pfl//lWgers Arch. Eur. J. Physiol.* 338:93–114.

Schwoch, G., and H. Passow. 1973. Preparation and properties of human erythrocyte ghosts. *Mol. Cell. Biochem.* 2:197–218.

Shiga, T., N. Maeda, T. Suda, K. Kon, and M. Sekiya. 1979 *a*. The

decreased membrane fluidity of in vivo aged human erythrocytes. *Biochim. Biophys. Acta.* 553:84–95.

Shiga, T., N. Maeda, T. Suda, K. Kon, M. Sekiya, and S. Oka. 1979 *b*. A kinetic measurement of red cell deformability: a modified pipette technique. *JPN. J. Physiol.* 29:705–720.

Tillman, W., C. Levin, G. Prindul!, and W. Schroter. 1980. Rheological properties of young and aged erythrocytes. *Klin. Wochenschr.* 58:569–574.

Usami, S., and S. Chien. 1973. Shear deformation of red cell ghosts. *Biorheology.* 10:425–430.

Waugh, R., and E. V. Evans. 1979. Thermoelasticity of red blood cell membrane. *Biophys. J.* 26:115–131.

Waugh, R., and P. L. LaCelle. 1980. Abnormalities in the membrane material properties of hereditary spherocytes. *J. Biomech. Eng.* 102:240–246.

Weed, R. I., P. L. LaCelle, and E. W. Merrill. 1969. Metabolic dependence of red cell deformability. *J. Clin. Invest.* 48:795–809.

Williams, A. R., and D. R. Morris. 1980. The internal viscosity of the human erythrocyte may determine its lifespan in vivo. *Scand. J. Haematol.* 24:57–62.